Journal of Applied Mechanics and Technical Physics, Vol. 35, No. 5, 1994

FEATURES OF THE CHANGE IN THE FREQUENCY SPECTRUM OF ELECTROMAGNETIC RADIATION DURING THE FRACTURE OF ROCK SPECIMENS

G. I. Kulakov and G. E. Yakovitskaya

UDC 622.831

The interest shown in the electromagnetic radiation (EMR) which — along with acoustic emission — accompanies the cracking of rocks is due to the large amount of information that can be obtained by studying this process and the broad possibilities for making practical use of the findings to monitor and predict the cracking and fracture (in earthquakes, shock bumps, and other dynamic phenomena) of rock masses [1, 2].

The main parameters by which a situation is judged to be critical are the number of pulses, their amplitude and frequency [3, 4], the distribution of the radiation with respect to energy level, and — most recently — the spectral characteristics of radiation from cracks, changes in these characteristics, and the change in the frequency corresponding to the maximum spectral density of the signal [5]. It was shown in [5, 6] that the latter change can be represented as consisting of three stages. The range corresponds to high frequencies in the first stage of defect growth. It shifts to a region of lower frequencies as the load increases. It again corresponds to high frequencies in the third stage, and there are subsequently fluctuations throughout the frequency range.

Such variation of the maximum spectral component of the signal is satisfactorily described by an S-shaped curve plotted from the line characterizing the maximum spectral components. The appearance of the second high-frequency maximum on the curve can be regarded as a predictive indicator of fracture.

It was shown in [7] that the value corresponding to the largest of the spectral amplitude maxima is found at the peak of the amplitude curve.

Our goal here is to use spectrum-time matrices to analyze the sequence of displacements of the maximum spectral components of the signal as the load (time t) increases.

The experimental method used in [8] included the loading of cylindrical specimens in uniaxial compression. The specimens, 46-59 mm in diameter and 70-90 mm in height, were composed of rocks and ores from the Tashtagol iron-ore deposit. Strips of a dielectric material were placed between the press platens and the specimens. The loading was done on a standard press exerting forces up to $5 \cdot 10^2$ kN at a rate of about 100 N/sec. The load was continuously increased until the specimen fractured.

Table 1 shows averaged mechanical characteristics of the rocks and ores (σ_{cn} is the strength in uniaxial compression, E is the elastic modulus, and ν is the Poisson's ratio). Also shown is the breaking load P recorded during loading of the specimens.

Several specimens of each type of rock were prepared for the tests. The average error of the mechanical parameters shown in the table is 15%.

The theoretical force acting on the specimen during loading was recorded by a standard extensometric method. The process of the nucleation and growth of microcracks and cracks was studied by recording electromagnetic radiation from the specimens. The radiation was recorded with the use of transducers consisting of magnetic mast-type and toroidal narrow-direction antennas placed about 0.02 m from the specimen.

The pulses of electromagnetic radiation generated during loading were received by the antennas and sent to the recording system (in the memory of a microcomputer) through a preamplifier.

It was observed during the experiments that the highest-amplitude pulses were generated at the moment the specimen fractured. The amplitudes of the recorded signals ranged from 20 to 75 μA/m.

Below, we examine experimental results obtained when we recorded the signals in two channels using two differently oriented antennas. We then subjected the signals to a spectral-time analysis by means of fast Fourier transforms (FFT). The

Novosibirsk. Translated from Prikladnaya Mekhanika i Tekhnicheskaya Fizika, No. 5, pp. 160-165, September-October, 1994. Original article submitted October 12, 1993; revision submitted December 28, 1993.

0021-8944/94/3505-0793$12.50

TABLE 1

No. of specimen	Specimen material	σ_{en}, MPa	$E \cdot 10^{-6}$, MPa	ν	P, kN
1	Marbleized limestone	67—109	0,36	0,23	$3 \cdot 10^2$
2	Magnetite ore	77—250	0,87	0,28	$1,5 \cdot 10^2$
3	Syenite 1	49—135	0,59	0,25	$2,4 \cdot 10^2$
4	Syenite 2	49—135	0,59	0,25	$1,4 \cdot 10^2$

TABLE 2

t, msec	$f \cdot 10^{-2}$, kHz																	
	25	29	33	38	42	50	57	66	74	85	98	112	128	147	168	192	220	252
	A, rel. units																	
17,00	683	726	729	744	784	801	789	778	740	670	585	494	344	250	240	457	435	400
17,78	691	737	741	762	803	830	829	820	816	763	704	643	525	269	162	427	427	435
18,86	699	748	753	782	838	861	874	886	886	868	839	809	749	627	554	480	347	365
19,93	704	755	761	795	855	881	900	920	933	933	923	900	882	830	810	704	516	524
20,95	708	761	766	804	868	825	919	943	966	981	981	978	972	963	949	919	863	849
21,75	709	762	767	807	872	899	924	949	976	996	998	996	993	998	993	980	967	961
21,90	709	763	766	807	872	899	426	950	977	991	999	998	993	1000	995	982	973	960
22,03	709	763	766	807	872	899	924	949	977	998	999	995	994	999	995	982	976	966
22,38	709	763	766	807	872	898	923	947	975	997	997	991	984	993	987	972	968	949
23,26	698	751	742	786	840	855	865	870	882	882	838	747	599	614	519	473	499	411
25,82	594	745	732	777	826	836	840	831	842	831	759	637	400	458	409	360	438	291
25,03	691	742	726	772	818	826	826	819	818	803	721	574	399	405	366	311	447	273
26,98	684	733	711	756	772	779	786	767	752	725	725	621	411	477	415	233	338	481
28,52	650	695	645	691	685	654	616	555	508	499	502	444	496	235	152	345	212	331
30,16	640	683	621	671	664	608	562	498	477	470	503	460	475	251	253	247	305	324

calculated data was organized into spectrum–time matrices having time intervals as the rows and frequency intervals as the columns. The resulting tables — printouts covering the period of time from the beginning of the loading process to complete fracture of the specimen (loss of continuity) — were referred to in [7] as EMR spectrum–time matrices. It was also noted in [7] that, in practice, it is more convenient to examine only the most informative part of the matrix (the truncated matrix).

The method used to analyze these matrices involved a line-by-line determination of the maximum spectral amplitudes and the use of these values to plot curves.

As an example illustrating the use of the method just described, Table 2 shows part of the spectrum-time matrix obtained for the EMR pulses generated in the loading of specimen 3 (syenite 1). We chose the maximum amplitude A = 1000 in constructing the matrix. The spectral amplitudes at all other points of the matrix were calculated in fractions of the maximum amplitude.

In connection with the problem of recording the EMR signals during the final stage of fracture (loss of continuity) and the corresponding reduction in the sensitivity of the recording equipment, no recording was made of microcrack nucleation and growth during the early stages of loading.

The matrix values were used to plot the curve of maximum spectral amplitude. Here, we chose the maximum spectral amplitude A_i. The corresponding points were connected in succession by segments of straight lines. The resulting stepped line begins with the maximum spectral amplitude $A_1 = 801$ at the frequency $f_1 = 0.50$ kHz in the first row of the matrix. It then shifts rightward to the region of higher frequencies, passes through the point with the largest amplitude maximum A = 1000 at f = 1.47 kHz, and subsequently shifts downward to the left in the matrix — gradually moving into the low-frequency region. The last point of this line corresponds to the maximum spectral amplitude A = 683 at f = 0.29 kHz.

The stepped line described above, showing a clear maximum in the coordinates t — f, characterizes the location of the points having the maximum spectral amplitudes within the EMR spectrum–time matrix. The line begins in the low-frequency region but shifts to a region of higher frequencies as the load increases. Here, the largest amplitude corresponds to a higher frequency — in the present case, the highest of all of the frequencies. The appearance of the highest-amplitude signal in the spectrum at the highest frequency corresponds to the final moment of formation of the main crack region in the loaded specimen. With further loading, the amplitudes decrease and shift to the region of lower frequencies. The stepped character of the amplitude lines was observed on a significant percentage of the volume of the rocks tested.

TABLE 3

t, msec	$f \cdot 10^{-2}$, kHz																	
	25	29	33	38	43	50	57	65	74	85	98	112	126	147	168	192	220	252
	A, rel. units																	
6,51	0	0	703	0	0	0	701	0	0	0	0	0	0	700	700	0	0	0
6,67	0	0	706	0	0	0	706	0	0	0	0	0	0	701	702	0	0	0
11,11	0	726	756	0	724	715	830	826	772	0	766	0	805	815	0	762	746	0
11,27	0	729	757	0	727	719	833	831	778	0	769	0	817	836	0	770	736	0
11,43	0	731	758	0	729	722	835	833	783	0	772	0	832	856	0	782	736	780
13,59	0	752	766	700	746	743	850	858	823	801	764	0	962	909	930	945	965	989
13,65	0	753	767	700	746	743	850	858	823	803	759	0	966	1000	920	941	961	991
13,80	0	754	767	0	746	743	850	856	823	806	754	0	970	999	923	935	954	986
14,45	0	757	767	0	746	739	846	851	817	807	727	0	977	983	872	874	895	936
14,60	0	758	767	0	745	737	845	849	814	806	719	0	979	976	850	850	876	919
18,84	0	746	743	0	0	0	751	0	0	0	0	0	968	0	0	0	0	0
19,05	0	745	742	0	0	0	746	0	0	0	0	0	742	0	0	0	0	0
19,16	0	744	740	0	0	0	742	0	0	0	0	0	725	0	0	0	0	0
19,25	0	742	738	0	0	0	737	0	0	0	0	0	708	0	0	0	0	0

TABLE 4

t, msec	$f \cdot 10^{-2}$, kHz																	
	378	390	401	414	426	439	453	466	481	495	510	526	542	559	575	593	611	630
	A, rel. units																	
14,14	763	763	765	765	763	754	741	723	712	704	0	0	0	0	725	771	793	784
14,60	821	823	877	830	830	827	821	813	807	803	800	797	797	805	825	843	845	823
14,75	864	869	875	880	884	887	888	889	879	879	880	882	882	893	901	903	892	859
14,92	895	902	910	916	921	925	927	928	930	933	936	942	947	952	951	947	928	887
15,08	914	922	931	938	944	950	953	956	959	963	969	976	983	987	986	974	950	905
15,24	920	929	938	946	953	959	963	966	969	973	978	987	994	1000	998	985	959	912
15,50	915	924	933	940	947	952	956	958	958	960	964	973	982	996	990	979	954	908
15,56	898	906	915	950	925	930	932	931	928	925	925	934	945	960	963	957	936	893
15,72	869	877	884	886	888	891	892	887	878	866	859	866	883	904	919	921	906	869
15,87	829	837	840	837	836	837	836	826	808	779	758	767	796	831	858	891	866	836
16,03	770	785	784	772	763	765	767	754	722	0	0	0	0	740	785	815	919	798

The structure of the line agrees satisfactorily with the S-shaped characteristic curve described in [6] for the crack process. This curve corresponds to the lower loop of the line (see Fig. 1).

Table 2 shows the maximum-amplitude line in the form of a symmetric stepped line. If the frequency change between columns of the matrix and the time interval between the rows of the matrix approach zero in the limit, the broken (stepped) line becomes a smooth curve with an extended peak. The character of this curve can be regarded as empirical proof of the existence of the S-curve introduced in [6].

However, the line symmetry just described was not fully present for some of the rock specimens we tested. Let us consider features of the structure of the lines for several of the most characteristic specimens (see Table 1). Specimen 1 — marbleized limestone, frequency range to 2.52 kHz, recording channel 1; Specimen 4 — syenite 2, frequency range to 5.04 kHz, recording channel 1; Specimen 2 — magnetite ore, frequency range to 6.3 kHz, recording Channel 2.

It should be noted that the electromagnetic radiation was recorded in the experiments by means of differently oriented, narrow-direction magnetic antennas and the information was recorded on a magnetic carrier in Channels 1 and 2. Tables 3-5 show the truncated spectrum-time matrices for the above-indicated specimens. Lines of maximum spectral amplitude were constructed for these specimens by the same method as shown in Table 2. Just as in Table 2, the lines begin in the low-frequency region, i.e. at a loading stage corresponding to more than 0.5 of the ultimate strength. High-amplitude, low-frequency signals are generated here. As the load then increases further, the maximum-amplitude lines shift to a higher frequency region (again as in Table 2) and pass through a point that has the largest of the maximum values (in our notation, A = 1000). The line subsequently returns to the low-frequency region.

However, in contrast to the maximum-amplitude line in Table 2, the lines shown in Figs. 3-5 have peaks with certain characteristic structural features. Let us discuss some of these features.

The line shown in Table 3 (Specimen 1) has a amplitude blip in a region of frequencies that is high relative to the frequencies at which the largest amplitudes were recorded. This blip precedes the appearance of A = 1000. After the attainment of A = 1000, the line moves to the low-frequency part of the spectrum.

TABLE 5

t, msec	$f \cdot 10^{-2}$, kHz																	
	13	16	19	24	30	35	46	58	71	89	110	137	180	212	263	327	406	504
	A, rel. units																	
6,67	0	0	0	0	0	0	0	0	757	782	0	0	0	0	0	0	733	768
6,98	0	0	0	0	0	0	0	0	765	793	0	724	0	0	0	722	772	837
7,30	0	0	0	0	0	0	0	0	772	801	702	741	0	0	0	776	760	825
7,62	0	0	0	0	0	0	0	700	777	806	724	751	0	0	708	820	787	0
7,94	0	0	0	0	0	0	0	704	781	808	742	768	0	0	752	846	0	835
8,25	0	0	0	0	0	0	0	707	784	807	754	772	0	0	775	847	0	776
8,56	0	0	0	0	0	0	0	710	785	804	762	769	0	0	780	815	0	1000
8,89	0	0	0	0	0	0	0	712	785	798	765	760	0	0	768	748	0	982
9,20	0	0	0	0	0	0	0	713	784	788	764	748	0	0	741	0	0	901
9,52	0	0	0	0	0	0	0	714	782	776	758	723	0	0	700	0	706	794
9,84	0	0	0	0	0	0	0	714	778	761	740	0	0	0	0	0	774	0

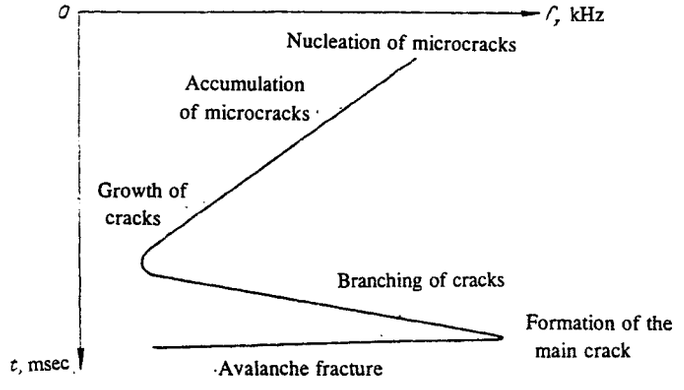

Fig. 1

The line in Table 4 (Specimen 2) also has a blip in the high-frequency region in advance of A = 1000. However, this line ends in the high-frequency region after the latter value of A is reached, rather than moving to the low-frequency region.

Yet another feature is seen in the structure of the peak on the line in Table 5 (specimen 4). In this case, there is a "dip" in the peak within the low-frequency region above A = 1000. Amplitude subsequently reaches its maximum value A = 1000 and the line moves to the low-frequency region.

Analyzing the overall changes in the spectral composition of the electromagnetic radiation at different loading stages, we note that the EMR spectrum is formed in the high-frequency part of the frequency range during the initial stage. Then, as the load increases, it shifts to the low-frequency part. This is illustrated by the top parts of Tables 2-5. A further increase in load is accompanied by an increase in the fraction of the high-frequency components in the signal spectrum, with a simultaneous shift in the maximum spectral amplitudes to the high-frequency region. This is illustrated by the middle part of Fig. 1 and Tables 2-5. The low-frequency components are joined by high-frequency components from the highest amplitude maximum, which is evidence of the formation of the main crack zone. The peak on the maximum-amplitude line may have different configurations, i.e. it may be extended (see Table 2), have "blips" or "dips," or may end after the high frequencies are reached (see Table 4). Finally, during the last loading stage, electromagnetic radiation is accompanied by a decrease inthe fraction of the high-frequency components and an increase in the fraction of the low-frequency components of the EMR signal. The specimen fracture process ends with the radiation of EMR pulses whose spectrum is usually concentrated in the low-frequency region.

Thus, the envelope of the lines of maximum spectral amplitude is the same for all of the test specimens in all of the tables. The envelope has the form of a loop that is extended parallel to the frequency axis, with the peak value being located in the high-frequency part of the frequency spectrum. An envelope of this nature corresponds to the lower part of the loop on the S-curve characterizing cracking and fracture.

The above experiments and an analysis of the literature data [5-7] on electromagnetic radiation accompanying the fracture of rocks permit the following conclusions:

— as the load increases, the overall changes in the spectral components of the EMR produce a successive displacement of the maximum spectral amplitude from the high-frequency to the low-frequency part of the spectrum; the maximum amplitude then returns to the high-frequency region and, finally, goes back to the low-frequency portion of the spectrum;

— the line of maximum spectral amplitude constructed on truncated EMR matrices corresponds to the second and third stages of the S-curve characterizing the fracture process [6];

— the concept of the S-curve is validated by the experiments described here and our analysis of the literature data. This analysis shows that the maximum spectral amplitude moves from the high-frequency to the low-frequency part of the spectrum as the load increases. After the load increases to a certain point, however, the maximum amplitude returns to the high-frequency region before ending up back in the low-frequency part.

This study was completed with the financial support of the Russian Fund for Basic Research (Grant No. 93-05-8642).

REFERENCES

1. Inquiry into Electromagnetic Precursors to Earthquakes, IFZ An SSSR (O. Yu. Shmidt Institute of Earth Physics of the Soviet Academy of Sciences), Moscow (1988).
2. P. V. Egorov, V. V. Ivanov, and L. A. Kolpakova, "Certain laws governing pulsed electromagnetic radiation from alkali-halide crystals and rocks," FTPRPI, No. 1, 67-70 (1988).
3. G. V. Afanasenko and I. M. Shvedov, "Study of natural and industrial electromagnetic fields to predict rock bursts during the mining of carnallite," FTPRPI, No. 1, 78-83 (1991).
4. B. I. Frid, A. N. Shabarov, V. M. Proskuryakov, et al, "Formation of electromagnetic radiation in a coal seam," FTPRPI, No. 2, 40-42 (1992).
5. M. V. Kas'yan, V. V. Robsman, and G. N. Nikogosyan, "Change in the emission spectrum during the cracking and fracture of rocks," Dokl. Akad. Nauk SSSR, **306**, No. 4, 826-830 (1989).
6. M. V. Kurlenya, G. E. Yakovitskii, and G. I. Kulakov, "Stages of the fracture process based on a study of electromagnetic radiation," FTPRPI, No. 1, 44-49 (1991).
7. M. V. Kurlenya, G. I. Kulakov, and G. E. Yakovitskaya, "Spectral-time analysis of electromagnetic radiation during the cracking of rock specimens," Ibid., No. 1, 3-13 (1993).
8. I. L. Gufel'd, N. N. Nikiforova, A. A. Rozhnoi, et al., "Characteristics of sources of electromagnetic radiation in a rock mass," in: Stress-Strain State of Rock Masses, IGD SO RAN (Mining Institute, Siberian Department of the Russian Academy of Sciences), pp. 70-76 (1988).